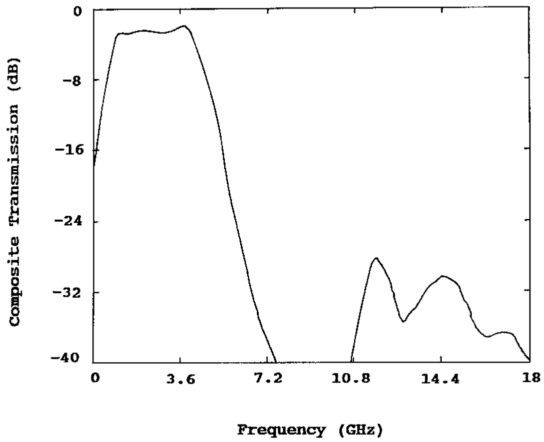

Fig. 4. Transmission data for the cascade structure involving two circulators (circulator #1).

Conclusion

Practical wide stopband filters involving asymmetric stripline Y-junction circulators have been fabricated and tested at microwave frequencies from 0.05 to 18 GHz. The calculated biasing field requirement, transmission frequency, insertion loss, isolation, and stopband frequency range are in reasonable agreement with the corresponding measured values. The ferrite filters were designed to operate away from magnetic resonance so that high power handling capability could be achieved. The fabricated filters show stopbands of 2 octaves and hence can be used extensively as protective elements in a wide frequency range in radome applications. The device's insertion loss can be further improved by using low loss ferrite materials or impedance matching networks to the input and output ports of the device. The passband of the device is wider than theoretically expected. However, the wide transmission band implies increased thermal stability of the device and ease of operation when deployed in a cascade configuration.

References

[1] P. Roeschmann, "YIG filters," *Philips Tech. Rev.*, vol. 32, p. 322, 1971.
[2] H. How, G. Vittoria, and C. Carosella, "Novel filter design incorporating asymmetrical stripline Y-junction circulators," *IEEE Trans. Microwave Theory Tech.*, vol. 39, pp. 40–46, Jan. 1991.
[3] D. K. Linkhart, *Microwave Circulator Design.* Norwood, MA: Artech House, 1989.
[4] L. D. Landau and E. M. Lifshitz, *Electrodynamics of Continuous Media.* New York: Pergamon, 1982, p. 25.

Some Observations on the Design and Performance of Distributed Amplifiers

J. L. B. Walker

***Abstract*—This paper presents closed-form analytic expressions for the voltage and power distribution along the drain line of an ideal distributed amplifier.**

Manuscript received April 23, 1991; revised August 15, 1991.
The author is with Thorn EMI Electronics Limited, Sensors Group, Manor Royal, Crawley, W. Sussex RH10 2PZ England.
IEEE Log Number 9103892.

I. Introduction

A recent paper [1] reports on a computer analysis of a distributed amplifier and shows that a nonuniform power distribution occurs in the drain line, and that over some portions of the frequency band one or more of the active devices may become passive i.e. absorb power rather than generate it. It is the purpose of this paper to present closed-form analytic expressions for the voltage and power distribution along the drain line of an ideal lossless distributed amplifier and to show that the above conclusions are fundamental to its operation.

II. Analysis of an Ideal Distributed Amplifier

An ideal GaAs FET has an equivalent circuit of just a gate-source capacitance C_{gs} at its input, and a voltage-controlled current generator g_m in parallel with a capacitance C_{ds} at its output. Fig. 1 shows an idealized distributed amplifier in which each FET has been replaced by this equivalent circuit. Physically, each gate-source capacitance is symmetrically embedded between a pair of inductors $L_g/2$ and forms a Tee-type constant K filter section [2]. However, the ensuing analysis is simplified if one considers the inductance L_g to be symmetrically embedded between a pair of capacitors $C_{gs}/2$; thus each gate-to-source capacitance C_{gs} in Fig. 1 is represented as two capacitors $C_{gs}/2$ in parallel. Similarly, each drain-to-source capacitance is represented as two capacitors $C_{ds}/2$ in parallel. The Pi type constant K filter section has an image impedance and propagation constant of

$$Z_\pi^g = Z_0^g \Big/ \sqrt{1 - \left(\frac{\omega}{\omega_{cg}}\right)^2} \tag{1}$$

and

$$\theta_g = \cos^{-1}\left(1 - 2\left(\frac{\omega}{\omega_{cg}}\right)^2\right) \tag{2}$$

respectively, where

$$Z_0^g = \sqrt{\frac{L_g}{C_{gs}}} \tag{3}$$

and

$$\omega_{cg} = 2/\sqrt{L_g C_{gs}}. \tag{4}$$

The cascade of constant K filter sections forms an artificial transmission line of characteristic impedance Z_π^g. This transmission line needs to be terminated in source and load impedances of Z_π^g in order that $S_{11} = 0$. If the input and output half-sections are included, then the transmission line needs to be terminated in Z_T^g [2] rather than Z_π^g for $S_{11} = 0$ where

$$Z_T^g = Z_0^g \sqrt{1 - \left(\frac{\omega}{\omega_{cg}}\right)^2}. \tag{5}$$

Assuming, for the moment, that $C_{\text{add}} = 0$ in Fig. 1, then all the preceding equations apply to the drain line also if the subscript or superscript g is replaced everywhere by d.

Now for proper operation of the distributed amplifier one requires [3]

$$\theta_g = \theta_d = \theta \tag{6}$$

and hence, from (2)

$$\omega_{cg} = \omega_{cd} = \omega_c. \tag{7}$$

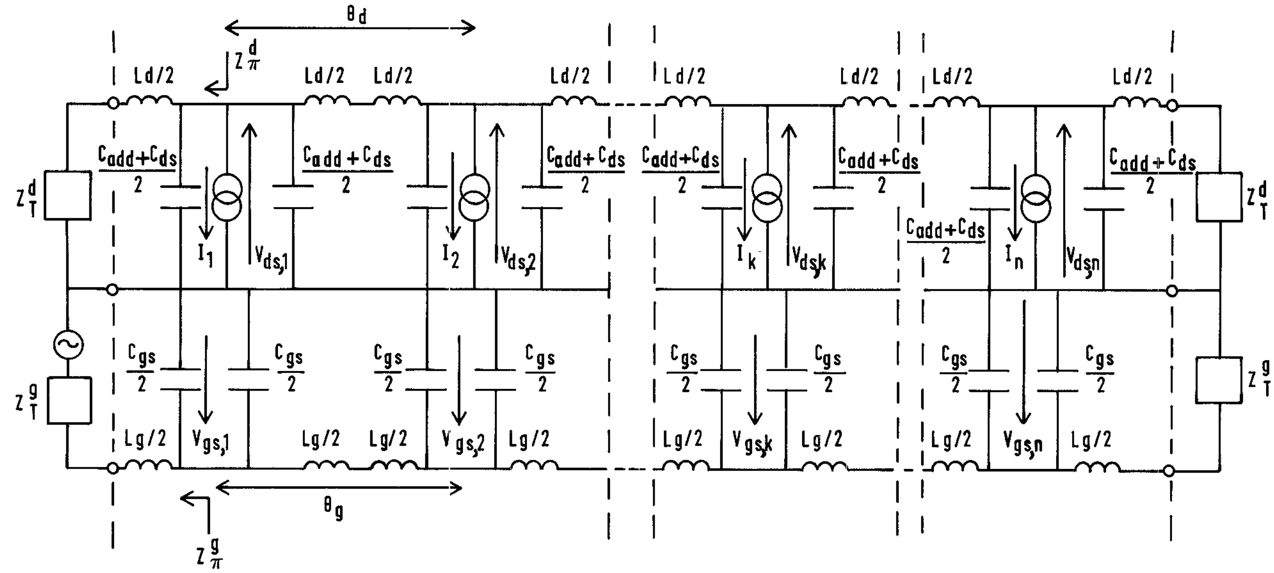

Fig. 1. Circuit diagram of ideal distributed amplifier.

Normally one also requires

$$Z_T^g = Z_T^d = Z_T \tag{8}$$

and thus

$$\left.\begin{aligned} Z_\pi^g &= Z_\pi^d = Z_\pi \\ Z_0^g &= Z_0^d = Z_0 \end{aligned}\right\}. \tag{9}$$

Equations (3), (4), (7), and (9) together imply that one requires

$$\begin{aligned} L_g &= L_d \\ C_{gs} &= C_{ds}. \end{aligned} \tag{10}$$

However, for all GaAs FET's $C_{gs} > C_{ds}$ and hence it will be assumed in the following that some additional capacitance to ground C_{add} is added at the drain of each FET, as shown in Fig. 1, so that

$$\begin{aligned} C_{gs} &= C_{ds} + C_{\text{add}} = C \\ L_g &= L_d = L. \end{aligned} \tag{11}$$

There are, of course, other methods of satisfying (6) and (8) apart from adding extra capacitance at the drain such as the use of a series gate capacitance [4]. This technique might be preferred in practical applications.

Each FET injects a current of $g_m V_{gs,i}$ into the drain line. Since the drain of each FET sees an impedance of Z_π in both directions, half of this current travels to the left and half to the right. The voltage at the drain of each FET is readily calculated by replacing the left- and right-hand sections of the drain line by their Norton equivalents. Thus the drain-to-source voltage across the kth FET is given by

$$V_{ds,k} = Z_\pi/2\{I_1 e^{-j(k-1)\theta} + \cdots I_{k-1}e^{-j\theta} + I_k + I_{k+1}e^{-j\theta} + \cdots I_n e^{-j(n-k)\theta}\}. \tag{12}$$

Now

$$I_k = g_m V_{gs,1} e^{-j(k-1)\theta} \tag{13}$$

where $V_{gs,1}$ is the gate-to-source voltage across the first FET, thus

$$V_{ds,k} = \frac{Z_\pi}{2} g_m V_{gs,1} \sum_{i=1}^{n} e^{-j\{i-1+|k-i|\theta\}}. \tag{14}$$

This series can be assumed in closed-form as

$$V_{ds,k} = \frac{Z_\pi}{2} g_m V_{gs1} e^{-j(k-1)\theta} \cdot \left\{k + \frac{e^{-j2\theta} - \exp\left[-j2(n-k+1)\theta\right]}{1 - e^{-j2\theta}}\right\}. \tag{15}$$

Straightforward but lengthy trigonometric manipulations show that $|V_{ds,k}|$ is given by

$$|V_{ds,k}| = \frac{Z_\pi}{2} g_m V_{gs,1} \sqrt{k^2 + \frac{2k\cos(n-k+1)\theta \sin(n-k)\theta}{\sin\theta} + \frac{\sin^2(n-k)\theta}{\sin^2\theta}}. \tag{16}$$

The voltage distribution along the drain line as given by the above expression is plotted in normalized form for the case $n = 4$ in Fig. 2 from which it can be seen that a very large variation in the magnitude of the drain-to-source voltage with frequency occurs for the FET's nearest the input. However, it can be shown from (16) that at all frequencies

$$|V_{ds,k}| \geq |V_{ds,(k-1)}|, \quad k = 2 \to n. \tag{17}$$

Thus the voltage variation with frequency must progressively decrease as k increases since $|V_{ds,n}/(Z_\pi/2) g_m V_{gs,1}|$ is a constant.

Since the largest drain-to-source voltage is that of the last FET, the linear output power from the distributed amplifier is maximized when

$$|V_{ds,n}| = \frac{V_{dgB} - V_p - V_t}{2} \tag{18}$$

where V_{dgB} is the gate-drain breakdown voltage, V_p is the pinch-off voltage and V_t is the knee voltage. Under these conditions the maximum linear output power from the distributed amplifier is given

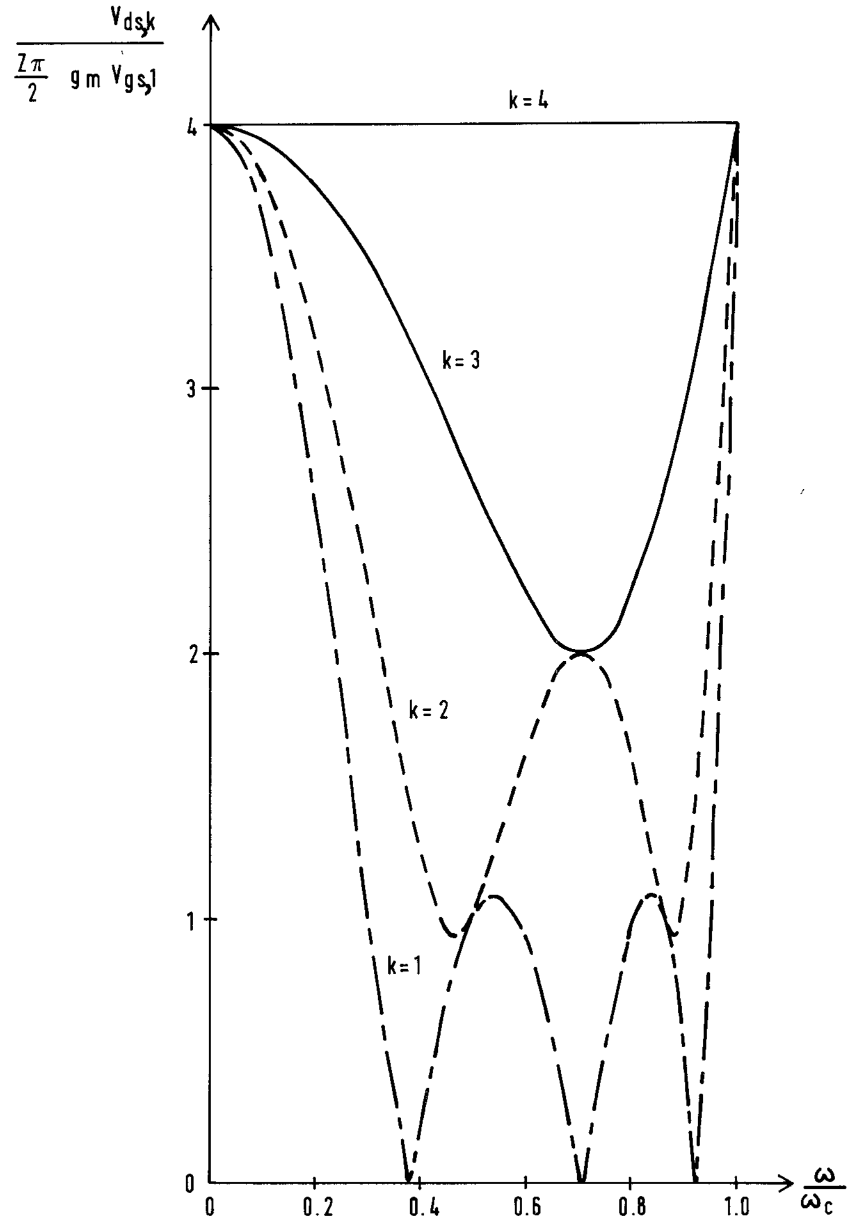

Fig. 2. Voltage distribution along the drain line for $n = 4$.

by

$$P_{max} = \frac{(V_{dgB} - V_p - V_t)^2}{8Z_\pi}. \quad (19)$$

Regardless of the number of FET's used P_{max} is the maximum linear output power from a distributed amplifier having the topology shown in Fig. 1 and is determined principally by V_{dgB} and Z_π. Thus the linear power output and efficiency of the distributed amplifier are half that achievable from lossless power combining of the individual FET's. For a typical FET having $V_{dgB} = 20$ V, $V_p = 2.5$ V and $V_t = 1$ V, then $P_{max} = 0.68$W if $Z_\pi = 50\ \Omega$. The gate widths of the individual FET's should be chosen such that their saturated drain current is given by

$$I_{dss} = 2(V_{dgB} - V_p - V_t)/nZ_\pi. \quad (20)$$

For the example given above $I_{dss} = 0.66/n$A.

The power generated by each FET is given by

$$P_k = \tfrac{1}{2}\,\mathrm{Re}\,(V_{ds,k} I_k^*). \quad (21)$$

Making the necessary substitutions from (13) and (15) and simplifying, we find

$$P_k = Z_\pi (g_m V_{gs,1})^2 \left\{ k + \frac{\cos\,(n - k + 1)\theta \,\sin\,(n - k)\theta}{\sin\,\theta} \right\}. \quad (22)$$

The power generated by each FET as given by the above expression is plotted in normalized form for the case $n = 4$ in Fig. 3. Also plotted in Fig. 3 in normalized form is the sum of the power dissipated in the load and in the drain line dummy load given by

$$P_T = \frac{Z_\pi}{8} (g_m V_{gs,1})^2 (n^2 + (\sin n\theta/\sin \theta)^2). \quad (23)$$

A number of observations can be made about the distribution of power generation. Firstly, as can be seen from Fig. 3, over a small

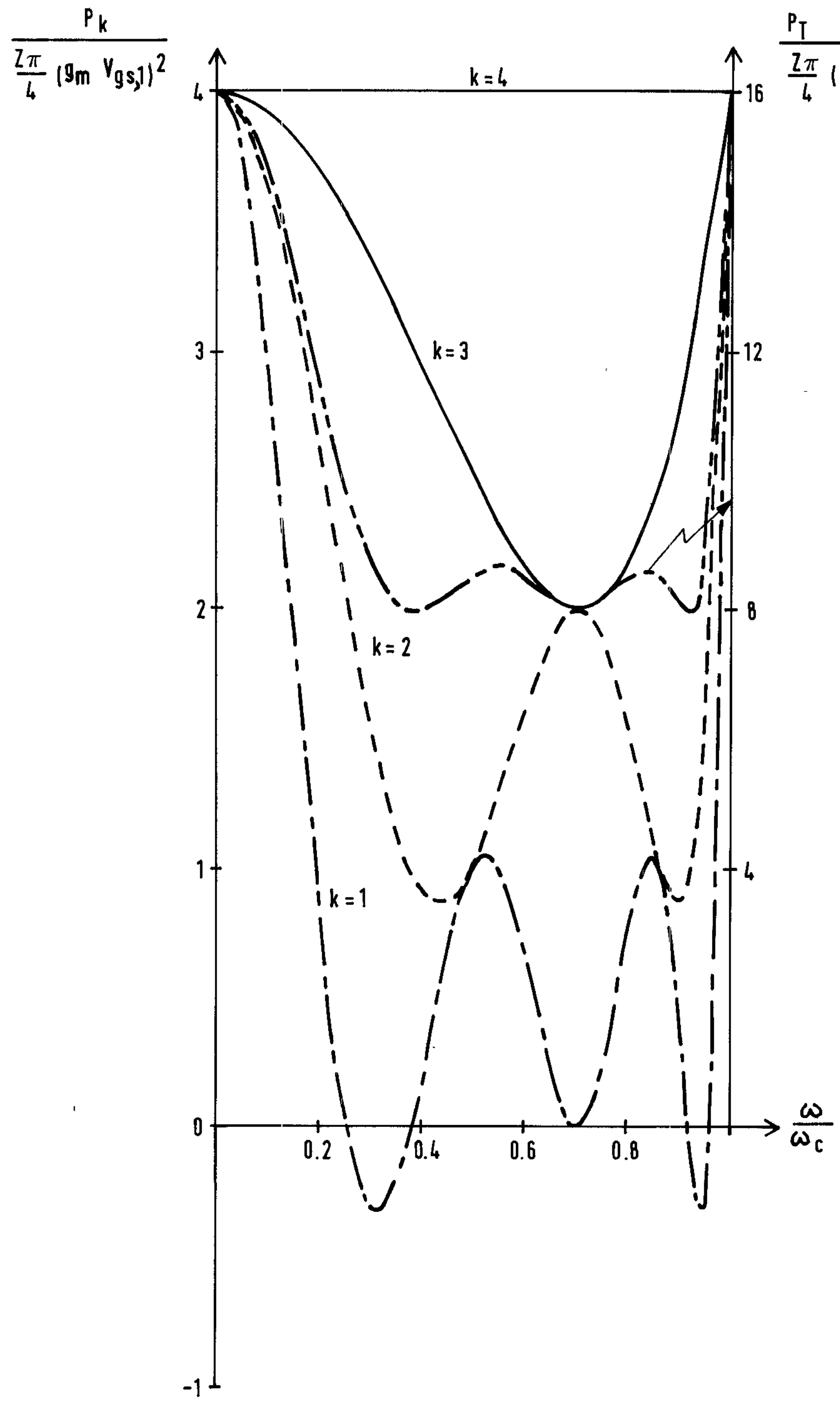

Fig. 3. Total power dissipated in external loads and power distribution along the drain line for $n = 4$.

range of frequencies the first FET actually absorbs power. This is contrary to the statement made by Niclas *et al.* [1] that "owing to the absence of any power dissipating parasitics and feedback elements in the transistor's simplified model, no negative energy flow exists in the idealized active devices." This surprising result, which has been independently verified using Touchstone®, is a consequence of the fact that the voltage at any point on the drain line depends upon the vector addition of the various current components at that point as shown by (12), and thus the voltage across an FET can be in phase with the current flowing through it. Secondly, it can be shown from (19) that

$$P_k \geq P_{k-1}, \quad k = 2 \rightarrow n \tag{24}$$

and hence the variation with frequency of the power generated by each FET must decrease as k increases since $P_n/(Z_\pi/4)\,(g_m V_{gs,1})^2$ is a constant. Thirdly, the last FET generates almost half the output power over most of the frequency range, i.e., $0.3 < \omega/\omega_c < 0.95$; the third FET contributes never less than 25% of the output power over the same frequency range whilst the first FET contributes at

®A registered trademark of EEsof, Inc., Westlake Village, CA.

most 12% and generally much less than this. The second FET, of course, makes up the balance.

Finally, an alternative but entirely equivalent way of interpreting the above analysis is to consider the load line seen by each FET [5]. Each FET has the same current swing but very different magnitudes and phases of voltage swing which are frequency dependent with the result that each FET operates along a different load line. As observed by Salib *et al.* [5] the load line the FET operates along is the electronic load line not the circuit element value of $Z_\pi/2$.

III. Conclusion

Closed-form analytic expressions for the voltage and power distribution along the drain line of an ideal distributed amplifier have been presented. It has been shown that the power generation is very nonuniform and that some FET's may actually absorb power rather than generate it over a portion of the frequency band.

References

[1] K. B. Niclas, R. R. Pereira, and A. P. Chang, "On power distribution in additive amplifiers," *IEEE Trans. Microwave Theory Tech.*, vol. 38, pp. 1692–1700, Nov. 1990

[2] G. Matthaei, L. Young, and E. M. T. Jones, *Microwave Filters, Impedance-Matching Networks, and Coupling Structures*. New York: McGraw-Hill, 1964.

[3] C. S. Aitchison, "The intrinsic noise figure of the MESFET distributed amplifier," *IEEE Trans. Microwave Theory Tech.*, vol. MTT-35, pp. 460–466, June 1985.

[4] Y. Ayasli, S. W. Miller, R. Mozzi, and L. K. Hanes, "Capacitively coupled travelling-wave power amplifier," *IEEE Trans. Microwave Theory Tech.*, vol. MTT-32, pp. 1704–1709, Dec. 1984.

[5] M. L. Salib, D. E. Dawson, and H. K. Hahn, "Load-line analysis in the frequency domain with distributed amplifier design examples," in *IEEE MTT-S Int. Microwave Symp. Dig.*, June 1987, pp. 575–578.

A Convergence Acceleration Procedure for Computing Slowly Converging Series

Surendra Singh and Ritu Singh

***Abstract*—The application of sloped θ-algorithm to the partial sums of a slowly converging series is shown to accelerate its convergence. The algorithm is applied to accelerate the convergence of series representing the free-space periodic Green's functions involving the zeroth-order Hankel function of the second kind, and its associated Fourier transform. Numerical results indicate that the algorithm converges faster than the Shanks' transform. It is also able to sum the series to machine precision in about 20 terms. A relative error measure is shown as a function of the number of terms of various combinations of source and observation points. The relative saving in computation time is also provided to show the benefit of using the algorithm.**

I. Introduction

In the numerical solution of problems involving a periodic geometry, one is usually faced with repeated evaluations of an infinite series represented the Green's function. The Green's function series converges very slowly. Hence, a significant amount of computer CPU time is spent in repeated computations of such series. One way to solve the problem of slow convergence of the series is to transform it into another series which in turn converges faster than the original series. The transformation then becomes the key to success or failure in achieving the accelerated convergence. Acceleration techniques employed so far make use of Kummer's transformation in conjunction with Poisson summation formula [1], [2], and Shank's transform [3]. In this paper we report the use of θ-algorithm [4], [5] in accelerating the convergence of free-space periodic Green's functions involving a single infinite summation. The algorithm is simple to implement and is shown to perform better than Shank's transform [6].

Manuscript received May 13, 1991; revised September 12, 1991.

The authors are with the Department of Electrical Engineering, The University of Tulsa, Tulsa, OK 74104.

IEEE Log Number 9104480.

II. θ-Algorithm

Let S_n be the partial sum of n terms of a series such that $S_n \to S$ as $n \to \infty$, where S is the sum of the series. The θ-algorithm can be computed as follows with the even order terms given by

$$\theta_{2k+2}^{(n)} = \theta_{2k}^{(n+1)} + \frac{[\theta_{2k}^{(n+2)} - \theta_{2k}^{(n+1)}][\theta_{2k+1}^{(n+2)} - \theta_{2k+1}^{(n+1)}]}{[\theta_{2k+1}^{(n+2)} - 2\theta_{2k+1}^{(n+1)} + \theta_{2k+1}^{(n)}]},$$

$$k = 0, 1, 2, \cdots \tag{1}$$

and the odd order terms by

$$\theta_{2k+1}^{(n)} = \theta_{2k-1}^{(n+1)} + \frac{1}{[\theta_{2k}^{(n+1)} - \theta_{2k}^{(n)}]}, \qquad k = 0, 1, 2, \cdots \tag{2}$$

where

$$\theta_{-1}^{(n)} = 0, \quad \theta_0^{(n)} = S_n. \tag{3}$$

The even order terms, $\theta_{2k+2}^{(n)}$, give estimates of S whereas the odd order terms, $\theta_{2k+1}^{(n)}$, are merely intermediate quantities. The algorithm can be illustrated by applying it to the slowly converging series for $ln2$:

$$ln2 = \sum_{m=1}^{\infty} \frac{(-1)^{m+1}}{m}.$$

As indicated, the series converges to $ln2 = 0.6931471$. The results of applying the θ-algorithm to the sequence of partial sums $S_1, S_2, \cdots, S_{10}$ are given in Table I. The algorithm converges to seven significant digits (one digit less than the number of digits carried in the partial sum).

III. Free-Space Periodic Green's Functions

The Green's function for a one-dimensional array of phase shifted line sources located at (x', y') in each unit cell and spaced d units apart along the y axis is given by

$$G = \frac{1}{4j} \sum_{m=-\infty}^{+\infty} e^{-jk_y md} H_0^{(2)}(k[(x - x')^2 + (y - y' - md)^2]^{1/2}) \tag{4}$$

where $H_0^{(2)}(\cdot)$ is the zeroth-order Hankel function of the second kind, k is the wavenumber of the medium, k_y is the inter-element phase shift, and the coordinates (x, y) locate the observation point. The spatial domain Green's function in (4) converges very slowly for all combinations of source and observation points. The Fourier transform of (4) gives the spectral domain Green's function given by

$$G = \sum_{m=-\infty}^{\infty} \frac{1}{j2dk_{x_m}} \exp(-jk_{x_m}|x - x'|) \cdot \exp[-j(k_y + 2m\pi/d)(y - y')], \tag{5}$$